Article

Cell Reports

NEIL3-Dependent Regulation of Cardiac Fibroblast Proliferation Prevents Myocardial Rupture

Graphical Abstract

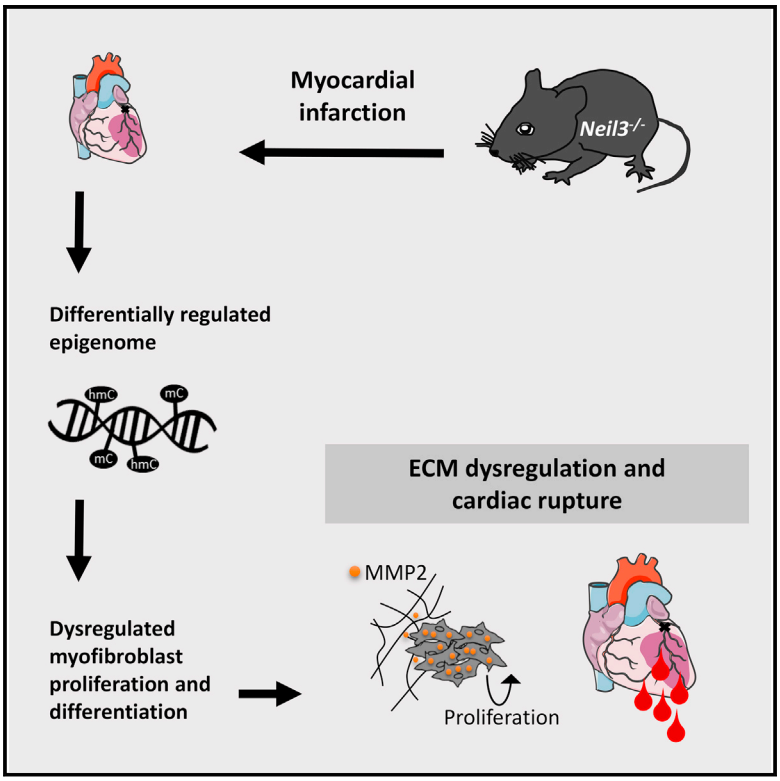

Authors

Maria B. Olsen, Gunn A. Hildrestrand, Katja Scheffler, ..., Pål Aukrust, Magnar Bjørås, Alexandra V. Finsen

Correspondence

magnar.bjoras@ntnu.no

In Brief

Olsen et al. show that the DNA repair enzyme, NEIL3, has impact on survival after myocardial infarction in mice. They find that NEIL3 regulates cardiac fibroblast proliferation and thereby affects extracellular matrix modulation. They propose that NEIL3 operates by regulating DNA methylation of genes important for fibroblast proliferation and differentiation.

Highlights

- NEIL3, a DNA repair enzyme, modulates DNA methylation
- Mice lacking NEIL3 have higher risk of cardiac rupture after myocardial infarction
- *Neil3*$^{-/-}$ hearts show no hypermutator phenotype or genome instability
- NEIL3 fine-tunes proliferation of cardiac fibroblasts

Olsen et al., 2017, Cell Reports *18*, 82–92
January 3, 2017
http://dx.doi.org/10.1016/j.celrep.2016.12.009

OPEN ACCESS
CellPress

Cell Reports
Article

NEIL3-Dependent Regulation of Cardiac Fibroblast Proliferation Prevents Myocardial Rupture

Maria B. Olsen,[1,9,10,16] Gunn A. Hildrestrand,[2,16] Katja Scheffler,[15,16] Leif Erik Vinge,[1,3,9] Katrine Alfsnes,[1,9,10] Vuk Palibrk,[15] Junbai Wang,[6] Christine G. Neurauter,[2] Luisa Luna,[2] Jostein Johansen,[13] Jonas D.S. Øgaard,[1] Ingrid K. Ohm,[1,9] Geir Slupphaug,[12,15] Anna Kuśnierczyk,[12,15] Arnt E. Fiane,[5] Sverre-Henning Brorson,[6] Lili Zhang,[8] Lars Gullestad,[1,3,9] William E. Louch,[8,9] Per Ole Iversen,[4,11] Ingunn Østlie,[6] Arne Klungland,[2] Geir Christensen,[3,8,9] Ivar Sjaastad,[3,8,9] Pål Sætrom,[13,14,15] Arne Yndestad,[1,9,10] Pål Aukrust,[1,7,10] Magnar Bjørås,[2,15,17,*] and Alexandra V. Finsen[1,3,9]

[1]Research Institute of Internal Medicine
[2]Department of Microbiology
[3]Department of Cardiology
[4]Department of Haematology
[5]Department of Cardiothoracic Surgery
[6]Department of Pathology
[7]Section of Clinical Immunology and Infectious Diseases
[8]Institute for Experimental Medical Research
Oslo University Hospital and University of Oslo, 0424 Oslo, Norway
[9]Center for Heart Failure Research
[10]K.G. Jebsen Inflammation Research Centre
[11]Department of Nutrition
University of Oslo, 0317 Oslo, Norway
[12]Proteomics and Metabolomics Core Facility–PROMEC
[13]Bioinformatics Core Facility–BioCore
[14]Department of Computer and Information Science
[15]Department of Cancer Research and Molecular Medicine
Norwegian University of Science and Technology, 7491 Trondheim, Norway
[16]Co-first author
[17]Lead Contact
*Correspondence: magnar.bjoras@ntnu.no
http://dx.doi.org/10.1016/j.celrep.2016.12.009

SUMMARY

Myocardial infarction (MI) triggers a reparative response involving fibroblast proliferation and differentiation driving extracellular matrix modulation necessary to form a stabilizing scar. Recently, it was shown that a genetic variant of the base excision repair enzyme NEIL3 was associated with increased risk of MI in humans. Here, we report elevated myocardial *NEIL3* expression in heart failure patients and marked myocardial upregulation of *Neil3* after MI in mice, especially in a fibroblast-enriched cell fraction. *Neil3*$^{-/-}$ mice show increased mortality after MI caused by myocardial rupture. Genome-wide analysis of 5-methylcytosine (5mC) and 5-hydroxymethylcytosine (5hmC) reveals changes in the cardiac epigenome, including in genes related to the post-MI transcriptional response. Differentially methylated genes are enriched in pathways related to proliferation and myofibroblast differentiation. Accordingly, *Neil3*$^{-/-}$ ruptured hearts show increased proliferation of fibroblasts and myofibroblasts. We propose that NEIL3-dependent modulation of DNA methylation regulates cardiac fibroblast proliferation and thereby affects extracellular matrix modulation after MI.

INTRODUCTION

It is estimated that every 44th second, a person in the United States suffers a myocardial infarction (MI) (Go et al., 2014). Although the management of these patients has markedly improved, the short- and long-term mortality, and in particular morbidity, is still high (Go et al., 2014). The reparative response after MI can typically be divided into three phases: an inflammatory phase involving infiltration of neutrophils and monocytes to remove damaged cells and tissue, a proliferative phase associated with neo-vascularization and proliferation and differentiation of fibroblast-like cells, and a maturation phase including extracellular matrix (ECM) synthesis leading to scar formation (Dobaczewski et al., 2010). Importantly, the repair process in the infarcted area involves a temporally regulated breakdown and deposition of ECM, and disturbances in this balance can have severe consequences, including cardiac rupture and ventricular aneurysm formation, as well as infarction expansion and maladaptive ventricular remodeling.

Ischemia and inflammation promote oxidative stress that may induce oxidative DNA damage (reviewed in Barzilai and Yamamoto, 2004). In addition, increased cell division during the proliferative phase strengthens the need for replication control in relevant cells such as (myo)fibroblasts. We have suggested that accumulation of DNA damage, especially oxidative DNA base modifications, may play a role in the cardiac repair and remodeling processes following MI (Yndestad et al., 2009). The degree of DNA damage, however, does not only depend on genotoxic events, but also on DNA repair mechanisms that are scarcely studied within the myocardium following MI.

The most important pathway for repair of DNA base lesions is the base excision repair (BER) pathway. BER is initiated by DNA glycosylases that remove modified bases leaving apurinic/apyrimidinic (AP) sites, which are further processed by an AP lyase and/or phosphodiesterases that remove the sugar-phosphate residue. DNA polymerase and DNA ligase complete the repair process (BER is reviewed in Krokan and Bjørås, 2013). Altered BER mechanisms seem to play a role in the pathogenesis of various disorders such as malignancies, HIV infection, neurodegeneration, and ischemic brain disorder (Aukrust et al., 2005; Canugovi et al., 2012; Dallosso et al., 2008; Sheng et al., 2012). In addition, we have shown myocardial activation of the BER pathway in a rat model of MI (Yndestad et al., 2009). The biological significance of BER activation following MI, however, remains unclear.

NEIL3 is a mammalian oxidized base-specific DNA glycosylase (reviewed in Liu et al., 2013). It has been shown to remove a broad spectrum of oxidative base lesions on single-stranded DNA substrates, indicating that NEIL3 serves to prevent accumulation of cytotoxic and mutagenic DNA lesions in mammalian cells (Krokeide et al., 2013; Liu et al., 2010, 2012). However, the function of NEIL3 seems to go beyond that of BER. The expression patterns of *NEIL3* mRNA in various human tumor tissues, in murine hematopoietic tissues and tissues that harbor stem cells in the brain, and during embryonic development in mice, as well as observations made in neural stem cells from mice, suggest that NEIL3 plays a role in the regulation of cell proliferation (Hildrestrand et al., 2009; Regnell et al., 2012; Reis and Hermanson, 2012; Rolseth et al., 2013; Torisu et al., 2005). Indeed, it has been shown that NEIL3 is upregulated in early S phase in various human cell lines, supporting a function of NEIL3 in replication-associated repair (Neurauter et al., 2012). Recently, it was reported that a genetic variant of human *NEIL3* was associated with increased risk of MI (Skarpengland et al., 2015). Based on these findings, we hypothesized that NEIL3 plays a role in myocardial repair and remodeling following MI. In order to test this hypothesis, we measured the myocardial expression of *NEIL3* in clinical samples from heart failure (HF) patients and studied wild-type (WT) and *Neil3*$^{-/-}$ mice in an experimental mouse model of MI.

RESULTS

Myocardial Expression of *NEIL3* Is High in Patients with HF and Is Reduced after Implanting a Left Ventricular Assist Device

We first examined the myocardial *NEIL3* mRNA expression in clinical HF by comparing *NEIL3* levels in non-failing left ventricle (LV) obtained from six organ donors with *NEIL3* levels in the failing LV from eight patients with HF, before and after implantation of a left ventricular assist device (LVAD) (Figure 1A). *NEIL3* expression was markedly increased in HF patients compared with controls. Furthermore, the improvement in hemodynamic and neurohormonal parameters observed during LVAD treatment (median follow-up time of 8 months, range 1–18 months) was accompanied by a significant reduction in *NEIL3* expression. In contrast, expression of *NEIL1* and *NEIL2*, the two other known NEIL glycosylases, were either downregulated (*NEIL2*) or unchanged (*NEIL1*) in HF patients, and none of these glycosylases were significantly influenced by LVAD treatment (Figure 1A).

Time-Dependent and Cell-Specific Regulation of *Neil3* Expression in Mice following MI

To further examine the role of NEIL3 in myocardial repair and remodeling, we applied an experimental model of MI in mice. Myocardial *Neil3* mRNA expression was measured in WT mice 3, 7, and 21 days after permanent coronary artery ligation or sham operation (Figure 1B). *Neil3* was markedly upregulated in the infarcted as well as in the non-infarcted part of the LV compared with sham, with the most pronounced increase after 3 and 7 days. In contrast, the expression of *Neil1* and *Neil2* was only modestly altered (Figure 1B). Expression levels were clearly more moderate in sham samples than in MI samples, particularly after 3 days (Figure S1C). Thus, it is reasonable to assume that the early increase in *Neil3* expression following MI is only to a minor degree influenced by the operation procedure. A possible cell-specific regulation of *Neil3* following MI was investigated by measuring *Neil3* mRNA levels in four distinct cell populations within the heart (i.e., cardiomyocytes, leukocytes, endothelial cells, and fibroblast-like cells) isolated from the myocardium of MI and sham-operated mice 7 days after surgery (Figures 1C and S1E). The *Neil3* expression levels in cardiomyocytes and leukocytes did not differ significantly between MI and sham-operated mice. In contrast, MI induced a significant increase in *Neil3* expression in endothelial cells (2.7-fold) and particularly in the fibroblast fraction (4.6-fold) compared with sham-operated animals. Our findings revealed an early and marked myocardial upregulation of *Neil3* expression following MI, specifically in fibroblast-like cells, that differed significantly from the regulation of *Neil1* and *Neil2.*

Increased Mortality in NEIL3-Deficient Mice following MI

To study the impact of NEIL3 on myocardial infarction, we used a NEIL3 knockout (KO) mouse model. WT and *Neil3*$^{-/-}$ mice were subjected to permanent ligation of the left coronary artery, and mortality was monitored during a follow-up period of 20 weeks. Eighty-four percent and 60% of the *Neil3*$^{-/-}$ and WT mice, respectively, died during the follow-up period, reflecting substantially increased mortality in *Neil3*$^{-/-}$ mice compared with WT mice (Figure 2A). Most of the mice died during the first week, and autopsies revealed that the cause of death was myocardial rupture, regardless of genotype.

Similar Infarct Size and Degree of Post-MI Remodeling in NEIL3-Deficient and WT Mice

Given the early increase in myocardial rupture and mortality in the *Neil3*$^{-/-}$ mice, we asked whether they suffered greater

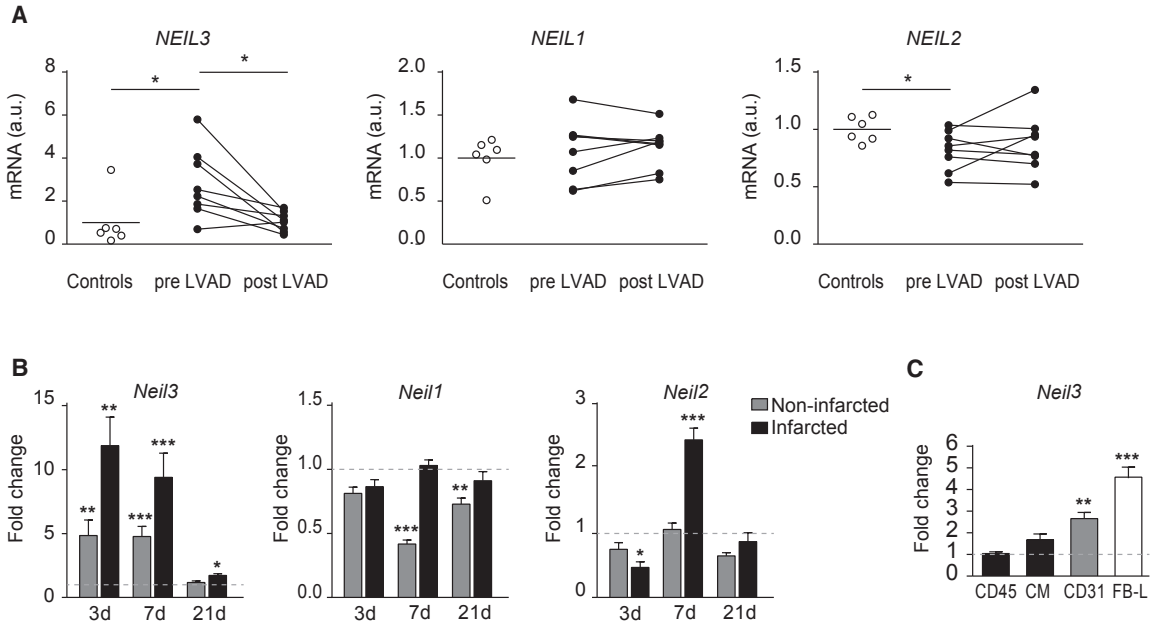

Figure 1. *NEIL3* Expression Is High in Patients with HF and in Fibroblast-like Cells from WT Mice after Induced MI

(A) *NEIL3*, *NEIL1*, and *NEIL2* mRNA expression in LVs from control hearts and from HF patients, before and after LVAD treatment. Relative quantity in HF patients (n = 8, closed symbols) compared with control patients (n = 6, non-failing myocardium, open symbols). Control values are normalized to 1.0 (indicated by horizontal lines). The difference in *NEIL3* expression between HF patients and controls was also significant when the two outliers (one patient and one control) were excluded (p = 0.006).

(B) *Neil3*, *Neil1*, and *Neil2* mRNA expression in non-infarcted and infarcted parts of LVs from mice subjected to MI at 3, 7, and 21 days after surgery. The graphs show fold change in MI samples relative to respective sham samples normalized to 1.0 (indicated by dashed lines). n = 5–8 mice, both sham and MI.

(C) *Neil3* expression in leukocytes (CD45), cardiomyocytes (CM), endothelial cells (CD31), and fibroblast-like cells (FB-L) isolated from LVs of sham and MI mice 7 days after surgery. The graph shows fold change in cell fractions isolated from MI mice relative to respective sham samples normalized to 1.0 (indicated by dashed line). n = 5 sham (2 sham CM [3 sham under detection limit]), n = 9 MI.

(B and C) Data are presented as mean + SEM.

*p ≤ 0.05, **p ≤ 0.01, ***p ≤ 0.001. See also Figure S1.

ischemic injury than WT mice after induction of MI. Magnetic resonance imaging (MRI) revealed, however, that the infarct size was equal in *Neil3*$^{-/-}$ and WT mice 1 day after infarction (Figure 2B). Next, morphometric and echocardiographic measurements were performed to elucidate possible differences in heart function between *Neil3*$^{-/-}$ and WT mice (Table S1). Three days post MI, both *Neil3*$^{-/-}$ and WT mice showed a significant and similar increase in LV weight (LVW) normalized for tibia length (LVW/TL), as a marker of LV hypertrophy, compared with sham. Although lung weight (LW) normalized for TL (LW/TL) was lower in *Neil3*$^{-/-}$ compared with WT following both sham and MI, the relative increase in LW/TL, a marker of congestive HF, was significant and similar in both genotypes following MI when compared with sham. Furthermore, the two genotypes displayed a similar degree of LV chamber dilatation and post-MI LV systolic dysfunction, as evaluated by LV fractional shortening (LVFS) and LV ejection fraction (LVEF). Together, these results imply that the increased mortality observed in *Neil3*$^{-/-}$ mice was not caused by a larger infarct area or by impaired LV function.

NEIL3-Deficient Hearts Display Unaltered Leukocyte Infiltration

Altered leukocyte infiltration could potentially promote myocardial rupture, influencing matrix degradation and fibrotic scar healing. Immunohistochemistry (IHC) of myocardial tissue, however, revealed similar levels of leukocytes, granulocytes, and macrophages in *Neil3*$^{-/-}$ and WT mice 3 days after MI, suggesting that altered leukocyte infiltration is not the cause of myocardial rupture in *Neil3*$^{-/-}$ mice (Figure S2).

NEIL3-Deficient Hearts Show No Increase in Steady-State Level of Oxidative DNA Base Lesions

Because NEIL3 is a DNA glycosylase known to repair oxidized base lesions, we expected to find increased oxidative DNA damage in the *Neil3*$^{-/-}$ animals. However, the levels of 8-oxoguanine (8-oxoG) and 5-hydroxycytosine (5-ohC), a substrate for NEIL3, did not differ between the two genotypes in any of the LV areas examined 3 days after MI (Figure S3A). The lack of increase in oxidative DNA damage in *Neil3*$^{-/-}$ mice did not reflect a compensatory upregulation of *Neil1* and/or *Neil2*, which also remove 5-ohC, in the LV of *Neil3*$^{-/-}$ mice (Figure S3B).

No Hypermutator Phenotype in NEIL3-Deficient Hearts

To investigate whether loss of NEIL3 is associated with increased mutation frequency predisposing to cardiotoxicity after MI, we applied whole-genome deep sequencing on DNA from non-infarcted LVs of WT and *Neil3*$^{-/-}$ hearts

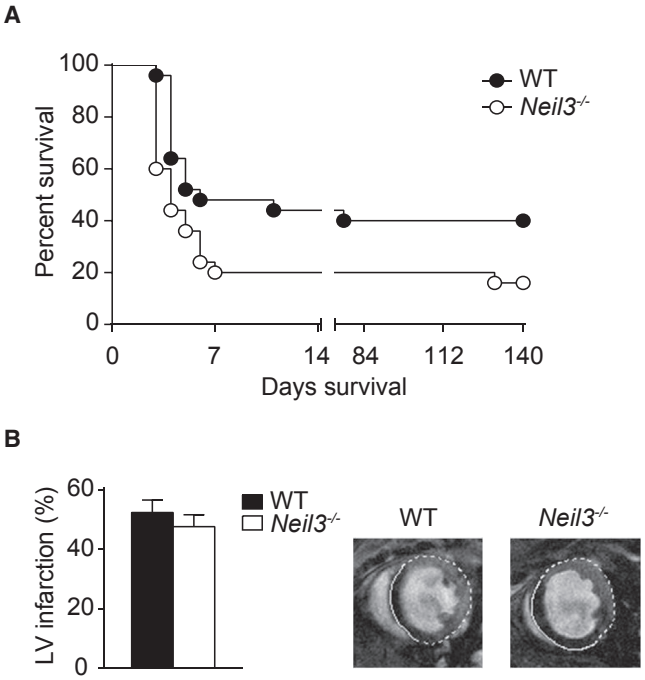

Figure 2. Increased Mortality in *Neil3*$^{-/-}$ Mice following MI

(A) Mortality rates in WT and *Neil3*$^{-/-}$ mice after induced MI. n = 25 mice per genotype. p = 0.02, by log-rank (Mantel-Cox) test.

(B) LV infarction size measured 1 day after induced MI by MRI. n = 5 WT and 7 *Neil3*$^{-/-}$.

Data are presented as mean + SEM. Representative images are shown.

3 days following MI. A DNA sequence variant analysis was performed using WT heart as reference genome. We found a modest increase in DNA variants genome-wide with 1,390 SNPs, 150 insertions, and 138 deletions that were evenly distributed across all chromosomes in *Neil3*$^{-/-}$ hearts (Figures 3A and 3B). Variants were detected in all genomic regions with the majority occurring in non-coding regions, e.g., intergenic regions and introns (Figure 3C). Analysis of base pair changes in SNPs showed the same distribution in WT and *Neil3*$^{-/-}$ hearts with C:G to T:A transitions being the most frequent, most likely because of deamination of 5-methylcytosine (5mC) and C to thymidine and uracil, respectively (Figure 3D). To identify a potential clustering of mutated genes in specific molecular pathways, we applied Ingenuity Pathway Analysis (IPA). We found that developmental processes, in particular of the nervous system, and processes involving cell-to-cell communication, cell growth and proliferation, and cell cycle regulation were significantly altered (Figure S4). These results suggest that although *Neil3*$^{-/-}$ hearts display no genome-wide hypermutator phenotype, they may accumulate mutations in specific genomic regions possibly affecting proliferation ability and function of (myo)fibroblasts after MI. Furthermore, it may indicate that these regions have altered chromatin structure leading to increased mutagenesis caused by transcriptional or epigenetic differences in *Neil3*$^{-/-}$ hearts.

RNA Sequencing Reveals Dysregulated Genes Related to Cardiovascular Development and Connective Tissue Disorders in NEIL3-Deficient Hearts

To further understand the processes occurring in the infarcted hearts of *Neil3*$^{-/-}$, we performed RNA sequencing on myocardial tissue harvested 3 days post MI. Differentially expressed genes (DEGs) in *Neil3*$^{-/-}$ mice were identified by comparing non-infarcted and infarcted LVs from *Neil3*$^{-/-}$ mice with respective samples from WT mice. We found 64 and 117 DEGs in the *Neil3*$^{-/-}$ non-infarcted and infarcted LVs, respectively, compared with WT (Figure 4A). Twenty-six of the DEGs were common for the non-infarcted and infarcted LVs, but the majority of DEGs (91) were regulated specifically in the infarcted LVs (Figure 4B). To identify diseases and biological processes that were influenced by NEIL3 deficiency, we used the IPA software. The top 10 disease-related categories affected in *Neil3*$^{-/-}$ hearts after MI involved "cardiovascular system development and function" and "connective tissue disorders" (Figure 4C). The regulation of the 27 DEGs annotated to the cardiovascular system development and function category are listed in Figure 4D.

MMP2 Dysregulation in NEIL3-Deficient Hearts

One network that was significantly regulated in the infarcted *Neil3*$^{-/-}$ tissue was the "cancer, organismal injury and abnormalities, and cardiovascular disease" network, and central in this network is matrix metalloproteinase-2 (MMP2; Figure S5). We observed a decrease in *Mmp2* expression following MI in WT mice, possibly because of less cardiomyocytes, which was not seen in *Neil3*$^{-/-}$ mice (Figure 5A). Hence both the RNA sequencing analysis and the qRT-PCR revealed a 2-fold increase in *Mmp2* mRNA levels in the infarcted *Neil3*$^{-/-}$ hearts compared with WT hearts 3 days post MI (Figures 4D and 5A). In line with this, we found a 1.7-fold increase in total MMP2 activity (p = 0.06; Figure 5A). The *Mmp2* mRNA levels correlated positively with *Collagen 1* and *3* mRNA levels in both infarcted (Figure 5C) and non-infarcted (Figure S6A) tissues, indicating that fibroblast-like cells are the producers of the increased *Mmp2* levels. Accordingly, increased *Mmp2* transcription was also observed in cultivated fibroblasts derived from *Neil3*$^{-/-}$ mice (Figure 5B). Collagen staining of the infarcted hearts did not reveal any differences between the genotypes (Figure S6C). Three days post MI is, however, very early with regard to fibrotic deposition; thus, the effects of the differently expressed genes with regard to fibrosis might first be detectable at a later time point.

NEIL3-Deficient Fibroblasts and Myofibroblasts Display a Higher Proliferation Rate Than Cells Derived from WT Mice

Our findings so far suggested that an altered (myo)fibroblast function could contribute to the increased mortality in *Neil3*$^{-/-}$ mice following MI. During post-MI repair, fibroblast-like cells are induced to proliferate and differentiate into myofibroblasts. Fibroblasts and myofibroblasts have important roles in the ECM homeostasis and could indeed be the link between altered matrix regulation *and* increased early mortality and LV rupture in *Neil3*$^{-/-}$ mice. The proliferation phase in mice typically starts around day 3 following MI. At this time point, in

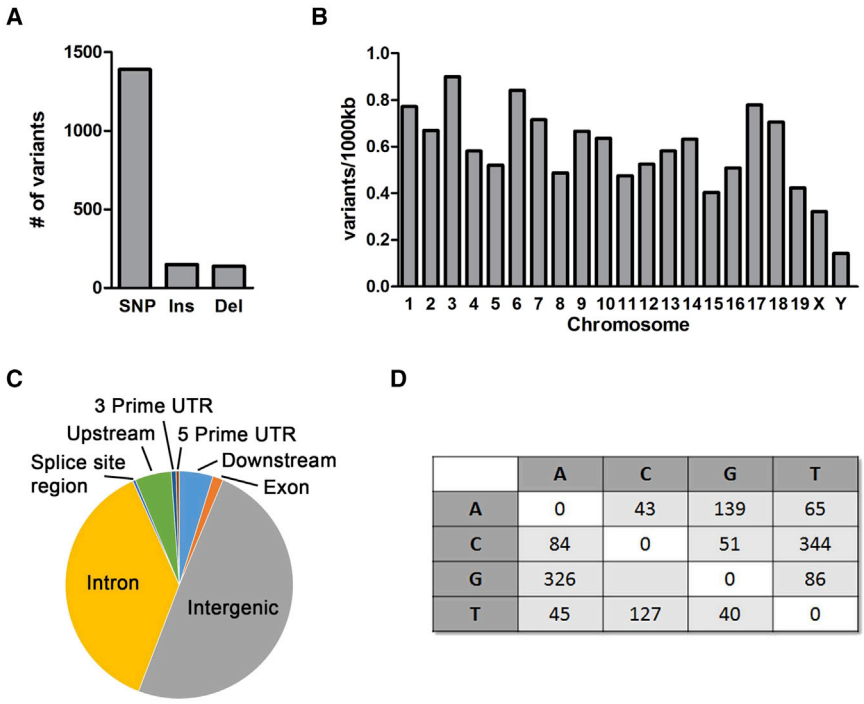

	A	C	G	T
A	0	43	139	65
C	84	0	51	344
G	326		0	86
T	45	127	40	0

Figure 3. Loss of NEIL3 in Heart Is Not Associated with a Hypermutator Phenotype

Whole-genome sequencing was performed on non-infarcted LVs of WT and *Neil3*$^{-/-}$ hearts 3 days after induced MI, followed by variant analysis using WT as reference. Four samples of DNA from each genotype were pooled before sequencing.

(A) DNA sequence variants.

(B) Chromosomal distribution of DNA sequence variants.

(C) Genomic region distribution of DNA sequence variants.

(D) Base changes count of SNPs.

Del, deletions; Ins, insertions. See also Figure S4.

accordance with elevated *Collagen* mRNA levels (Figure S6B), *Neil3*$^{-/-}$ hearts showed significantly increased expression of the myofibroblast markers *ASMA* and the splice variant of *fibronectin*, *fibronectin EDA* (Figure 6A). These results suggest that *Neil3*$^{-/-}$ hearts harbor more cells differentiating into myofibroblasts than WT hearts after MI. In order to examine (myo)fibroblast proliferation further, we subjected hearts isolated from mice that died of rupture 3–5 days after MI to IHC. Fibroblast proliferation, as assessed by co-staining with the proliferation marker Ki67 and the mesenchymal cell marker Vimentin, increased 2-fold, and myofibroblast proliferation, as assessed by co-staining with Ki67 and ASMA (actin, alpha 2, smooth muscle, aorta), increased 3.6-fold at the infarction border zone of *Neil3*$^{-/-}$ mice as compared with WT (Figures 6B and 6C). The (myo)fibroblast staining was repeated with the mitotic marker PHH3 showing similar results with significantly increased levels of mitotic fibroblasts and myofibroblasts in the *Neil3*$^{-/-}$ mice (Figure S7). Moreover, when examining cultured cardiac fibroblasts derived from *Neil3*$^{-/-}$ and WT hearts, we found that bromodeoxyuridine (BrdU) incorporation was higher in the fibroblasts lacking NEIL3, both with and without transforming growth factor β (TGF-beta) stimulation (Figure 6D). Also, when introducing a scar to confluent cultured cells, the *Neil3*$^{-/-}$ fibroblasts reoccupied the uncovered plastic significantly faster than the WT fibroblasts, indicating increased proliferation and/or migration of *Neil3*$^{-/-}$ cells (Figure 6E).

Genome-wide Alterations of the DNA Methylome and Hydroxymethylome in NEIL3-Deficient Hearts after MI

Epigenetic DNA modifications such as 5-methylcytosine (5mC) and 5-hydroxymethylcytosine (5hmC) are key regulators of gene expression. NEIL3 has recently been identified as a reader of oxidized 5mC derivatives (Spruijt et al., 2013), and to elucidate whether NEIL3 modulates the cardiac epigenome, we applied whole-genome sequencing of 5mC and 5hmC (Gao et al., 2013) to non-infarcted and infarcted LVs of WT and *Neil3*$^{-/-}$ mice. The same number of methylated regions (MRs) was analyzed in four genomic regions, i.e., TSS (transcriptional start site), TES (transcriptional end site), gene body, and 5 Dis (5′ distant), in both non-infarcted and infarcted *Neil3*$^{-/-}$ and WT (Figure 7A). Subsequently, differentially methylated and hydroxymethylated regions (DMRs/DhMRs) were identified by pairwise comparison of MRs between *Neil3*$^{-/-}$ and WT. The highest numbers of DMRs and DhMRs were found in NEIL3-deficient non-infarcted LVs, 943 and 844, respectively, compared with 348 DMRs and 336 DhMRs in infarcted LVs (Figure 7B). In non-infarcted LVs, hypo-DMRs were most prominent, whereas hyper-DMRs prevailed in infarcted LVs in the four genomic regions. In contrast, we found the majority of MRs to be hyper-hydroxymethylated in *Neil3*$^{-/-}$ non-infarcted LVs and a significant depletion of hyper-DhMRs in infarcted tissue (Figure 7B). These findings indicate that loss of NEIL3 causes significant changes in the cardiac epigenome following MI. Next, DMRs and DhMRs were mapped to their nearby gene and IPA was applied. DMRs in non-infarcted LVs and infarcted LVs were enriched in the function annotations "gene expression," "cellular development," "cell death and survival," "cellular growth and proliferation," and "cellular movement" (Figure 7C). A similar enrichment of DhMRs in these function annotations was observed, however, only in non-infarcted LVs (Figure 7D). To investigate the potential impact of DMRs and DhMRs on gene expression, we compared the genes identified by epigenetic sequencing analysis with the DEGs from our transcriptional analysis. Surprisingly, we found only a minor overlap of around 3% for non-infarcted and infarcted LVs (data not shown). However, among the genes with DMRs and DhMRs, several were annotated as transcriptional regulators. In general the expression levels of transcription factors are kept low (Vaquerizas et al., 2009); thus, RNA sequencing may not detect differential expression of these genes. By screening the DEGs from *Neil3*$^{-/-}$ non-infarcted and infarcted LVs, we identified several

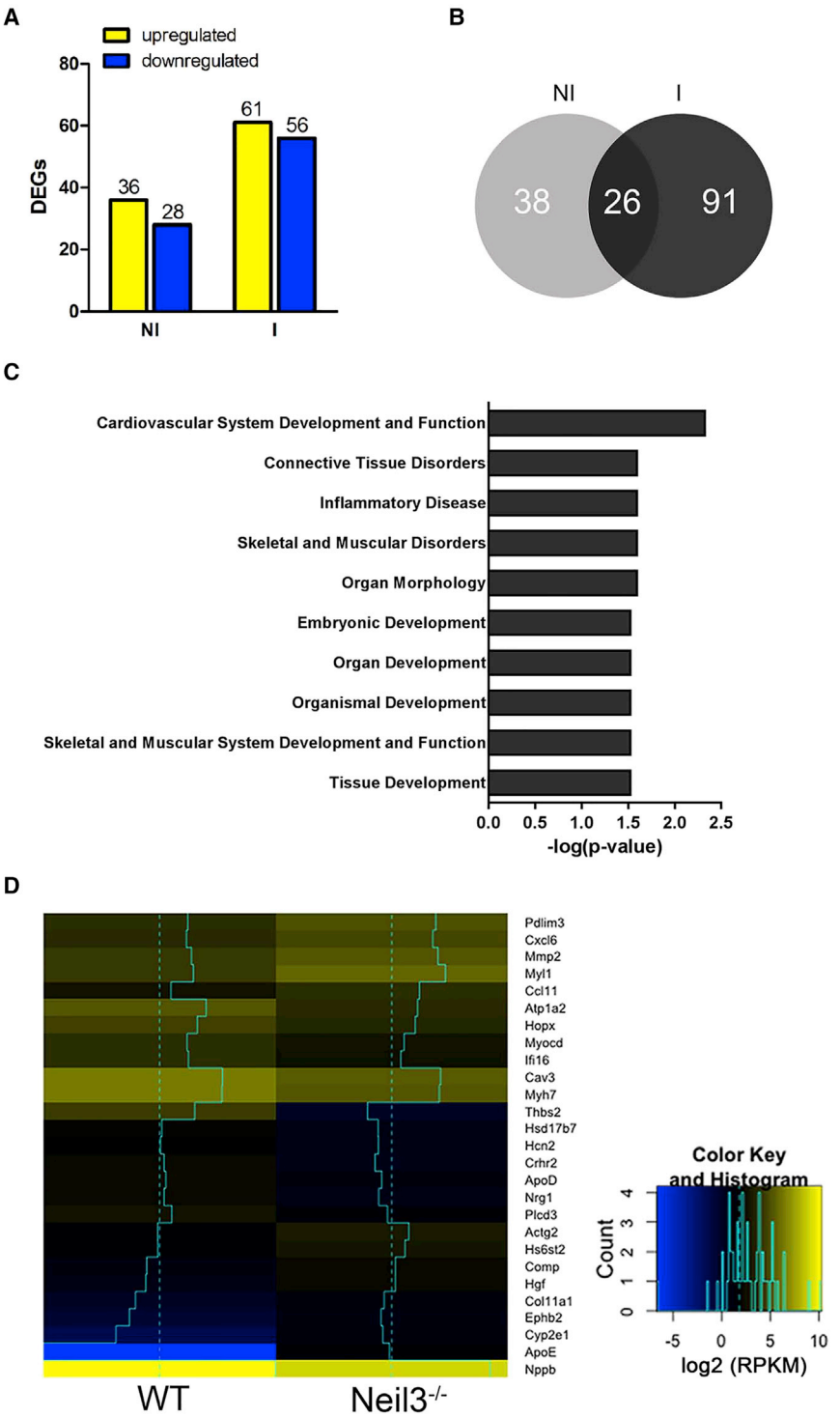

Figure 4. Transcriptome Analysis Revealed Enrichment of DEGs Involved in Cardiovascular Function in *Neil3*$^{-/-}$ Hearts after MI

RNA sequencing was performed on non-infarcted (NI) and infarcted (I) parts of LVs from WT and *Neil3*$^{-/-}$ hearts collected 3 days after induced MI. Three RNA samples from each genotype were pooled before sequencing.

(A) The number of DEGs that were significantly upregulated and downregulated in *Neil3*$^{-/-}$ cardiac tissue relative to WT.

(B) Venn diagram showing the overlap of DEGs from non-infarcted and infarcted cardiac tissue from *Neil3*$^{-/-}$ mice.

(C) Top 10 diseases and biological processes that are significantly enriched in DEGs from *Neil3*$^{-/-}$-infarcted cardiac tissue identified by IPA (p values by Benjamini-Hochberg multiple testing correction).

(D) Heatmap showing log2 transformed expression level of DEGs annotated to the "cardiovascular system development and function" category in (C). Count and number of genes with a given log2 reads per kilo base per million mapped reads (RPKM) value. The log2 RPKM values for each gene are indicated on the heatmap.

See also Figure S5.

genes that are known downstream targets of the transcriptional regulators with DMRs and DhMRs (Figure 7E). In particular, we identified DEGs from infarcted LVs (*Mmp2*, *Cyp2e1*, *Pdlim3*, *Nppb*, *Hgf*, *Myh7*, *Myl1*) that were also annotated to the "cardiovascular system development and function" category as presented in Figure 4D. These data suggest a role of NEIL3 as an epigenetic reader that modulates methylated regions of importance for the transcriptional response after MI.

DISCUSSION

We have previously shown that a certain NEIL3 variant may predispose to MI (Skarpengland et al., 2015) and that NEIL3 deficiency may promote atherosclerosis during a high-fat diet (Skarpengland et al., 2016). Herein, we report that NEIL3 deficiency also influences the consequences of MI. We found that the DNA glycosylase NEIL3 was highly upregulated in the hearts of both HF patients and post-MI mice. WT mice displayed an early and marked upregulation of *Neil3* mRNA following MI, predominantly in the fibroblast-enriched cell fraction, and NEIL3-deficient mice showed increased early mortality caused by myocardial rupture. Deep sequencing showed neither a hypermutator phenotype nor genomic instability in *Neil3*$^{-/-}$ hearts. Notably, whole-genome epigenetic sequencing of 5mC and 5hmC revealed a possible role of NEIL3 in epigenetic regulation of genes involved in the transcriptional response after MI. We propose that NEIL3 fine-tunes proliferation and differentiation of fibroblast-like cells following MI, and thereby matrix degradation and fibrogenesis within the myocardium. Thus, the marked

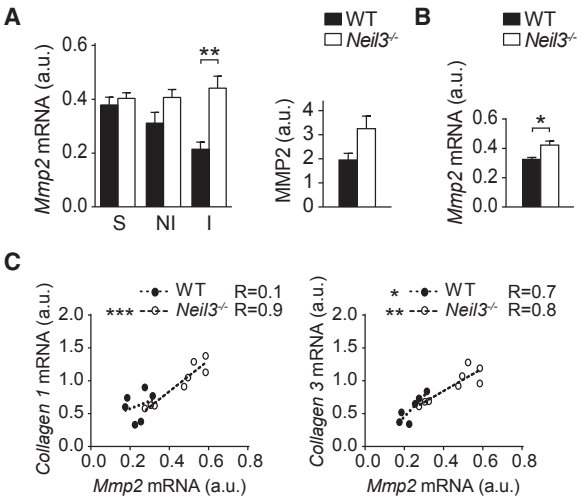

Figure 5. Correlative Upregulation of *Mmp2* and *Collagen 1* and *3* in *Neil3*$^{-/-}$ Hearts after MI

(A) *Mmp2*, measured by qRT-PCR, and total MMP2 protein levels, measured by zymography, in LV tissue collected 3 days after induced MI or sham operation. n = 6–9 mice per genotype for mRNA expression. MMP2 protein levels are relative to an internal loading control. n = 7 WT and 9 *Neil3*$^{-/-}$ for MMP2 protein measurements.

(B) *Mmp2* mRNA expression in cultivated myocardial fibroblasts isolated from naive WT and *Neil3*$^{-/-}$ mice. The cells were harvested 72 hr after treatment with TGF-beta. n = 4 mice per genotype.

(A and B) Data are presented as mean + SEM, and p values were obtained by comparing *Neil3*$^{-/-}$ samples with respective WT samples.

(C) Positive correlation between *Mmp2* mRNA expression levels and *Collagen 1* and *3* mRNA expression levels in infarcted *Neil3*$^{-/-}$ tissue after MI.

R^2 values are shown. *p ≤ 0.05, **p ≤ 0.01, ***p ≤ 0.001. I, infarcted part of LV; NI, non-infarcted part of LV; S, sham. See also Figures S1 and S6.

increase in myocardial *Neil3* mRNA expression early after MI in WT mice could represent a counteracting mechanism to prevent maladaptive ECM regulation.

DNA glycosylases are mainly known for initiating the BER pathway that protects cells from the mutagenic and/or cytotoxic effects of DNA base lesions. The NEIL DNA glycosylases recognize and remove a vast number of oxidized base lesions, with overlapping substrate specificity. Herein, we found that the genomic 8-oxoG and 5-ohC levels were similar in *Neil3*$^{-/-}$ and WT hearts after MI, suggesting that the steady-state level of oxidative DNA base lesions is not altered in NEIL3-deficient hearts. Furthermore, whole-genome deep sequencing displayed no hypermutator phenotype in NEIL3-deficient hearts, supporting that the genome stability is not altered in NEIL3-deficient hearts. We have previously shown that NEIL3 promotes proliferation of neuronal stem and progenitor cells in the mouse brain (Sejersted et al., 2011). In contrast, we show here that NEIL3 has a restrictive role on proliferation of cardiac fibroblasts and myofibroblasts. Cardiac fibroblasts are more or less quiescent during normal physiology, but are induced to proliferate upon stress such as MI. We previously reported repression of human NEIL3 in G_0-arrested cells and upregulation of NEIL3 both at the transcriptional and at the protein levels during S phase, again indicating that NEIL3 is mainly operating in proliferating cells (Neurauter et al., 2012). Thus, it is tempting to speculate that NEIL3 has a preference for or operates on specific genes or gene clusters in the genome that are important for regulation of cell cycle progression and that the mechanisms of action are at least partly cell specific (e.g., cardiac fibroblasts versus neuronal stem progenitor cells). Our findings herein suggest that such mechanisms could be of importance for the regulation of proliferation of fibroblast-like cells following MI.

A major finding in the present study is that NEIL3 deficiency significantly modulated the cardiac epigenome and that some of these modifications were also reflected in the cardiac transcriptional response following MI. Regulation of cellular morphology, movement, development, growth, and proliferation are all biological functions with great importance with regard to myofibroblast differentiation because cardiac myofibroblast precursors (i.e., fibroblasts, endothelial cells, epithelial cells, smooth muscle cells, and pericytes) all utilize these functions to some extent in order to change their morphology, migrate toward the infarcted area, proliferate, and promote wound healing (van den Borne et al., 2010). Accordingly, DNA methylation is known to be involved in myofibroblast differentiation (Neary et al., 2015; Watson et al., 2014; Xu et al., 2015). As the transdifferentiation process of myofibroblast precursors in general starts in the viable myocardium, it is not unexpected that the IPA pathway analysis showed the most prominent changes in this tissue. A recent study using pull-down experiments with oligos containing epigenetic methylation marks suggests that NEIL3 is a reader of 5hmC (Spruijt et al., 2013). Our data showing differential regulation of both 5mC and 5hmC in NEIL3-deficient hearts support that NEIL3 is affecting not only 5hmC levels, but the balance between epigenetic methylation of cytosine and oxidative demethylation. Thus, even though our analyses are not performed on cell-specific fractions, the pathway-specific DNA methylation patterns suggest that NEIL3 regulates proliferation and differentiation of fibroblast-like cells during MI repair, likely through regulation of epigenetic DNA methylation.

Cardiac rupture demonstrates the importance of balanced ECM degradation and restoration after MI (Gao et al., 2012), and a phenotype with increased rate of rupture, as shown here, indicates defective ECM regulation. Myofibroblasts are the main source of ECM and ECM modulators in the infarcted heart, and their behavior is extremely important for proper infarct healing. In the RNA sequencing analysis, "connective tissue disorders" was among the most significantly regulated disease categories. Herein, there are multiple regulated genes in the *Neil3*$^{-/-}$ hearts likely to affect ECM quality and therefore promote cardiac rupture. The role of MMP2, which is centrally placed in "the cancer and cardiovascular disease network," may be of particular importance because we found this gene/protein to be regulated in *Neil3*$^{-/-}$ infarcted tissue, and previous studies have shown decreased rupture rates after MI in MMP2-deficient mice (Matsumura et al., 2005). Moreover, the *Mmp2* mRNA level in infarcted *Neil3*$^{-/-}$ tissue was significantly increased and there was a 1.7-fold increase in total MMP2 protein level in the *Neil3*$^{-/-}$ hearts. Although the latter difference was not statistically significant (p = 0.06), the changes could still be biologically significant. Finally, the cardiac epigenetic modifications in NEIL3-deficient mice seemed also to involve MMP2 as a target,

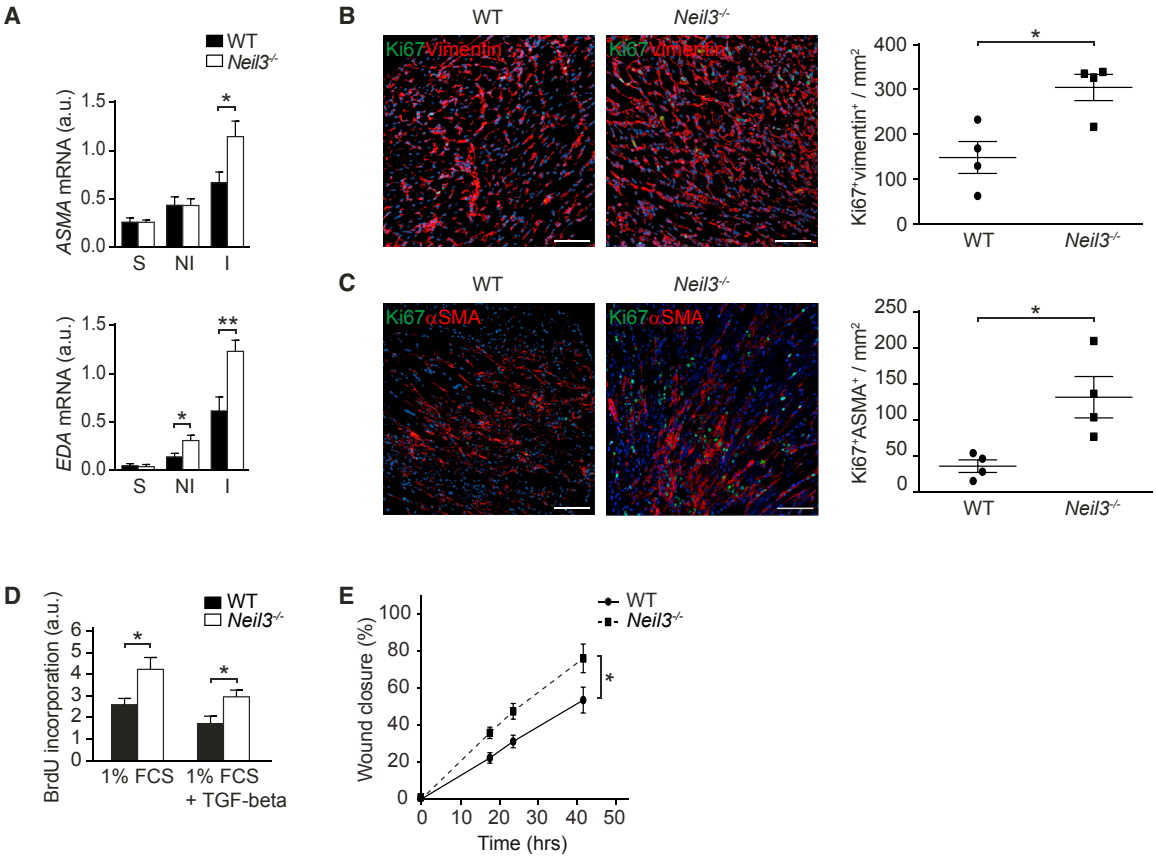

Figure 6. *Neil3*$^{-/-}$ (Myo)Fibroblasts Display Enhanced Proliferation Relative to WT Cells

(A) mRNA expression of the myofibroblast markers *ASMA* and *ED-A fibronectin* measured by qRT-PCR in LV tissue collected 3 days after induced MI or sham operation. n = 6–9 mice per genotype.

(B and C) Confocal images showing (B) Ki67- and Vimentin-positive cells and (C) Ki67- and ASMA -positive cells in border zones of the left ventricular wall isolated from WT and *Neil3*$^{-/-}$ mice that died 3–5 days after induced MI. Images represent projections of multiple confocal z sections. DAPI staining is shown in blue. Scale bars, 100 μm. Horizontal lines in graphs represent mean ± SEM. n = 4 mice per genotype.

(D) Cell proliferation measured in vitro by BrdU incorporation in cultured myocardial fibroblasts isolated from naive WT and *Neil3*$^{-/-}$ mice. Cells were cultivated in fetal calf serum (FCS), with (n = 4) or without TGF-beta (n = 6). Data are relative to the mean chemiluminescence of WT and *Neil3*$^{-/-}$ cells incubated in 0% FCS and presented as mean + SEM. Data are presented as mean + SEM.

(E) Wound closure as a function of time was compared in WT and *Neil3*$^{-/-}$ fibroblasts cultured in 0.1% FCS. n = 6 WT and 7 *Neil3*$^{-/-}$.

The p values were obtained by comparing *Neil3*$^{-/-}$ samples with respective WT samples (A–D); the p value was obtained by comparing the linear regression slope values (E). *p ≤ 0.05, **p ≤ 0.01. I, infarcted part of LV; NI, non-infarcted part of LV; S, sham. See also Figures S1 and S7.

further supporting this protease as a potential link between NEIL3 deficiency and early cardiac rupture.

The dysregulation of certain genes in the infarcted *Neil3*$^{-/-}$ hearts may indicate a compensatory response to loss of NEIL3 or it could be a direct consequence of lacking NEIL3 as a regulator, or a combination thereof. Balanced proliferation and differentiation of cells occur as a part of the infarction response in WT animals. Although not specific for MI, an imbalanced response could have deleterious consequences in the setting of MI, and we suggest that the increased proliferation seen in the *Neil3*$^{-/-}$ hearts could reflect a dysregulation of the infarction response, suggesting that NEIL3 operates as a brake, fine-tuning the level of proliferation. Thus, the increased proliferation of myocardial (myo)fibroblasts in mice lacking NEIL3 could not merely be a compensatory response, but rather an uncontrolled and dysregulated response to tissue damage following MI in *Neil3*$^{-/-}$ mice. Altogether, our results suggest that NEIL3-deficient hearts are less capable of fine-tuning the cell response to MI. This means dysregulated proliferation and differentiation of the fibroblast-like cells resulting in altered ECM regulation including increased MMP2 production followed by the fatal consequence: myocardial rupture.

To understand the molecular regulation of (myo)fibroblast proliferation and fibrogenesis is a major challenge in clinical medicine and is a prerequisite for the development of anti-fibrotic drugs, which are largely missing. Although induced proliferation of fibroblast-like cells is required after MI, an uncontrolled and imbalanced proliferation of these cells could promote ECM destabilization. Our findings suggest that NEIL3 could be an attractive target molecule in regulation of these processes, and further studies should explore the role of this DNA glycosylase in fibrosis regulation in other organs such as liver and lungs.

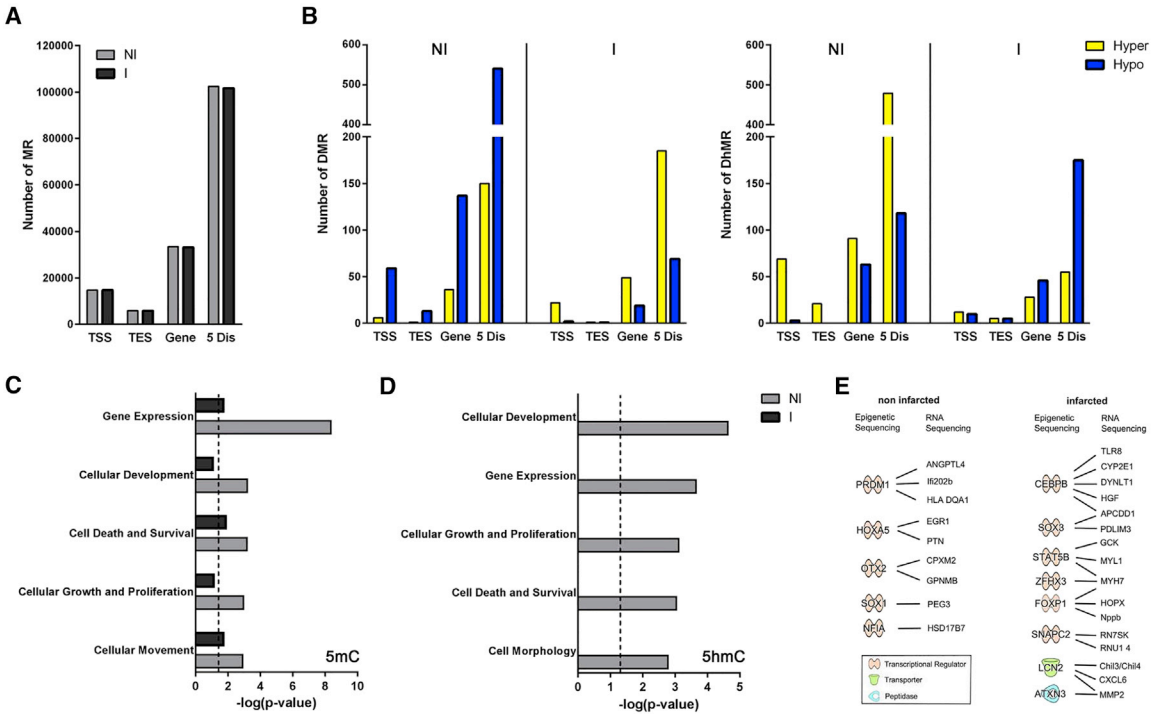

Figure 7. Loss of NEIL3 Modulates the Cardiac Epigenome after MI

HMST-seq was performed on non-infarcted (NI) and infarcted (I) parts of LVs from WT and *Neil3*$^{-/-}$ hearts collected 3 days after induced MI. Four DNA samples from each genotype were pooled before sequencing.

(A) The number of methylated regions (MRs) that were analyzed in both genotypes in four genomic elements.

(B) The number of hypo- and hyper-differentially methylated regions (DMRs) and hypo- and hyper-differentially hydroxymethylated regions (DhMRs) in the four genomic elements in *Neil3*$^{-/-}$ cardiac tissue compared with WT.

(C and D) Top molecular and cellular functions that are significantly enriched in (C) DMRs and (D) DhMRs from *Neil3*$^{-/-}$ hearts compared with WT as identified by IPA. Dotted line represents p = 0.05 by Benjamini-Hochberg multiple testing correction.

(E) Graphical illustration of transcriptional regulators with DMRs and DhMRs as identified by HMST-Seq and their known downstream targets identified as differentially expressed genes (DEGs) by RNA sequencing. Data were obtained by using the IPA software.

5 Dis, 5′ distant region; Gene, gene body; TES, transcription end site; TSS, transcription start site.

If the role of NEIL3 in regulation of fibroblast function is confirmed in other disease states, this molecule could represent a target for therapy in a wide spectrum of fibrotic disorders. Our findings also show a link between epigenetic and transcriptional regulation in NEIL3-deficient heart following MI, suggesting that NEIL3 is an epigenetic reader that modulates the transcriptional response after MI. Further studies on these issues could elucidate fundamental mechanisms linking environmental factors to cardiac disorders via modulation of epigenetics by oxidative DNA base lesion repair.

EXPERIMENTAL PROCEDURES

All material and methods are described in detail in the Supplemental Experimental Procedures.

Approvals

The clinical parts of this study were approved by the Regional Committee for Medical and Health Research Ethics (Permit number S-05172) and conducted according to the ethical guidelines outlined in the Declaration of Helsinki for use of human tissue and subjects. Informed written consent was obtained from all subjects. All animal experiments were approved by the Norwegian Animal Research Authority, and conducted in accordance with the laws and regulations controlling experimental procedures in live animals in Norway and the European Union's Directive 86/609/EEC.

Tissue Sampling from Human Myocardium

LV tissue from patients with advanced HF was sampled at the time of implantation and at the time of removal of a continuous-flow LV assist device (LVAD). Control human LV tissue was obtained from rejected donor hearts.

Mice

Neil3$^{-/-}$ mice were generated as previously described (Sejersted et al., 2011) and backcrossed for at least eight generations onto the C57BL/6 background.

Mouse Model of Experimental MI

MI was induced in 7- to 8-week-old mice as described previously (Finsen et al., 2005).

Cell Separation Protocol

Cardiac cells were isolated and separated as previously described (Ohm et al., 2014; Raake et al., 2008). Fibroblast-like cells equal a cell population in which cardiomyocytes, CD45^{+} cells, and CD31^{+} have been removed.

qRT-PCR

qRT-PCR was performed according to standard methods, and all calculations were done by using the standard curve method. Raw data are presented. *GAPDH* expression was determined for all samples analyzed (Figure S1).

MRI

MRI experiments were performed 1 day post MI with an MR system dedicated to mouse imaging.

LC-MS/MS Analysis of 8-Oxoguanine and 5-Hydroxycytosine in Genomic DNA

DNA from infarcted and non-infarcted parts of LVs harvested 3 days post MI was subjected to liquid chromatography-tandem mass spectrometry (LC-MS/MS) for 8-oxo-dG and 5-oh-dC detection.

Whole-Genome Deep Sequencing

Genomic DNA isolated from non-infarcted LVs of four WT and four *Neil3*$^{-/-}$ mice 3 days after MI was pooled and sent to BGI Tech Solutions, Hong Kong, for whole-genome sequencing. In the data analysis, strain-dependent variations were removed before *Neil3*$^{-/-}$-related mutations were detected.

RNA Sequencing

Total RNA from non-infarcted and respective infarcted LVs of three WT and *Neil3*$^{-/-}$ hearts was pooled and sent to BGI Tech Solutions, Hong Kong, for RNA sequencing and bioinformatics analyses.

Zymography

Protein homogenates were prepared from infarcted LV tissue of WT and *Neil3*$^{-/-}$ mice, harvested 3 days post MI.

Histology and Immunohistochemistry

Formalin-preserved, paraffin-embedded hearts from WT and *Neil3*$^{-/-}$ mice were sectioned and subjected to histology and IHC.

In Vitro Experiments on Cardiac Fibroblasts

Cardiac fibroblasts were isolated and cultivated (Ohm et al., 2014), and BrdU incorporation was measured by luminescence. Scrape wound was performed as previously described (Ohm et al., 2014).

Epigenetic Sequencing

Genomic DNA isolated from non-infarcted and infarcted LVs of four WT and four *Neil3*$^{-/-}$ mice 3 days after MI was pooled and sent to BGI Tech Solutions, Hong Kong, for hydroxymethylation- and methylation-sensitive tag sequencing (HMST-Seq) (Gao et al., 2013).

Statistical Analysis

GraphPad Prism version 6.02 (GraphPad Software) was used for designing graphs and for most statistical calculations. Both paired and unpaired, two-tailed t tests were used in Figure 1A. In Figures 1B and 2A the Mann-Whitney test and the log-rank (Mantel-Cox) test were applied, respectively. In Figures 4C, 7C, 7D, and S4 the IPA software and Benjamini-Hochberg multiple testing correction were used. In Figure 5C linear regression was applied, and in Figure 6E linear regression was applied for all individual samples, and *Neil3*$^{-/-}$ and WT slope values were compared. Unpaired, two-tailed t test was applied in all other figures. Results are considered significant when $p < 0.05$.

SUPPLEMENTAL INFORMATION

Supplemental Information includes Supplemental Experimental Procedures, seven figures, and one table and can be found with this article online at http://dx.doi.org/10.1016/j.celrep.2016.12.009.

AUTHOR CONTRIBUTIONS

Conceptualization, M.B.O., A.Y., P.A., M.B., and A.V.F.; Methodology, M.B.O., G.A.H., K.S., L.E.V., P.O.I., I.S., A.Y., M.B., and A.V.F.; Software, J.D.S.Ø.; Formal Analysis, M.B.O., G.A.H., K.S., J.J., G.S., A. Kuśnierczyk, and P.S.; Investigation, M.B.O., G.A.H., L.E.V., K.A., V.P., C.G.N., L.L., I.K.O., G.S., A. Kuśnierczyk, S.-H.B., L.Z., W.E.L., I.Ø., I.S., A.Y., and A.V.F.; Resources, A.E.F., L.G., and G.C.; Data Curation, K.S., J.J., P.S., and J.W.; Writing – Original Draft, M.B.O., G.A.H., P.A., M.B., and A.V.F.; Writing – Review & Editing, M.B.O., G.A.H., K.S., K.A., C.G.N., L.L., J.J., L.Z., L.G., W.E.L., P.O.I., A. Klungland, G.C., I.S., P.S., A.Y., P.A., M.B., and A.V.F.; Supervision, P.A., M.B., and A.V.F.; Funding Acquisition, A. Klungland, P.A., and M.B.

ACKNOWLEDGMENTS

This work was supported by grants from the Research Council of Norway, South-Eastern Norway Regional Health Authority, Norwegian Health Association, Anders Jahres Foundation, and Blix Foundation. The authors wish to acknowledge SERVIER Medical Art (www.servier.com) for use of their medical art kits when making the graphical abstract.

Received: June 8, 2016
Revised: October 6, 2016
Accepted: December 1, 2016
Published: January 3, 2017

REFERENCES

Aukrust, P., Luna, L., Ueland, T., Johansen, R.F., Müller, F., Frøland, S.S., Seeberg, E.C., and Bjørås, M. (2005). Impaired base excision repair and accumulation of oxidative base lesions in CD4+ T cells of HIV-infected patients. Blood *105*, 4730–4735.

Barzilai, A., and Yamamoto, K. (2004). DNA damage responses to oxidative stress. DNA Repair (Amst.) *3*, 1109–1115.

Canugovi, C., Yoon, J.S., Feldman, N.H., Croteau, D.L., Mattson, M.P., and Bohr, V.A. (2012). Endonuclease VIII-like 1 (NEIL1) promotes short-term spatial memory retention and protects from ischemic stroke-induced brain dysfunction and death in mice. Proc. Natl. Acad. Sci. USA *109*, 14948–14953.

Dallosso, A.R., Dolwani, S., Jones, N., Jones, S., Colley, J., Maynard, J., Idziaszczyk, S., Humphreys, V., Arnold, J., Donaldson, A., et al. (2008). Inherited predisposition to colorectal adenomas caused by multiple rare alleles of MUTYH but not OGG1, NUDT1, NTH1 or NEIL 1, 2 or 3. Gut *57*, 1252–1255.

Dobaczewski, M., Gonzalez-Quesada, C., and Frangogiannis, N.G. (2010). The extracellular matrix as a modulator of the inflammatory and reparative response following myocardial infarction. J. Mol. Cell. Cardiol. *48*, 504–511.

Finsen, A.V., Christensen, G., and Sjaastad, I. (2005). Echocardiographic parameters discriminating myocardial infarction with pulmonary congestion from myocardial infarction without congestion in the mouse. J. Appl. Physiol. *98*, 680–689.

Gao, X.-M., White, D.A., Dart, A.M., and Du, X.J. (2012). Post-infarct cardiac rupture: recent insights on pathogenesis and therapeutic interventions. Pharmacol. Ther. *134*, 156–179.

Gao, F., Xia, Y., Wang, J., Luo, H., Gao, Z., Han, X., Zhang, J., Huang, X., Yao, Y., Lu, H., et al. (2013). Integrated detection of both 5-mC and 5-hmC by high-throughput tag sequencing technology highlights methylation reprogramming of bivalent genes during cellular differentiation. Epigenetics *8*, 421–430.

Go, A.S., Mozaffarian, D., Roger, V.L., Benjamin, E.J., Berry, J.D., Blaha, M.J., Dai, S., Ford, E.S., Fox, C.S., Franco, S., et al. (2014). Heart disease and stroke statistics—2014 update: a report from the American Heart Association. Circulation *129*, e28–e292.

Hildrestrand, G.A., Neurauter, C.G., Diep, D.B., Castellanos, C.G., Krauss, S., Bjørås, M., and Luna, L. (2009). Expression patterns of Neil3 during embryonic brain development and neoplasia. BMC Neurosci. *10*, 45.

Krokan, H.E., and Bjørås, M. (2013). Base excision repair. Cold Spring Harb. Perspect. Biol. *5*, a012583.

Krokeide, S.Z., Laerdahl, J.K., Salah, M., Luna, L., Cederkvist, F.H., Fleming, A.M., Burrows, C.J., Dalhus, B., and Bjørås, M. (2013). Human NEIL3 is mainly a monofunctional DNA glycosylase removing spiroimindiohydantoin and guanidinohydantoin. DNA Repair (Amst.) *12*, 1159–1164.

Liu, M., Bandaru, V., Bond, J.P., Jaruga, P., Zhao, X., Christov, P.P., Burrows, C.J., Rizzo, C.J., Dizdaroglu, M., and Wallace, S.S. (2010). The mouse ortholog

of NEIL3 is a functional DNA glycosylase in vitro and in vivo. Proc. Natl. Acad. Sci. USA *107*, 4925–4930.

Liu, M., Bandaru, V., Holmes, A., Averill, A.M., Cannan, W., and Wallace, S.S. (2012). Expression and purification of active mouse and human NEIL3 proteins. Protein Expr. Purif. *84*, 130–139.

Liu, M., Doublié, S., and Wallace, S.S. (2013). Neil3, the final frontier for the DNA glycosylases that recognize oxidative damage. Mutat. Res. *743–744*, 4–11.

Matsumura, S., Iwanaga, S., Mochizuki, S., Okamoto, H., Ogawa, S., and Okada, Y. (2005). Targeted deletion or pharmacological inhibition of MMP-2 prevents cardiac rupture after myocardial infarction in mice. J. Clin. Invest. *115*, 599–609.

Neary, R., Watson, C.J., and Baugh, J.A. (2015). Epigenetics and the overhealing wound: the role of DNA methylation in fibrosis. Fibrogenesis Tissue Repair *8*, 18.

Neurauter, C.G., Luna, L., and Bjørås, M. (2012). Release from quiescence stimulates the expression of human NEIL3 under the control of the Ras dependent ERK-MAP kinase pathway. DNA Repair (Amst.) *11*, 401–409.

Ohm, I.K., Alfsnes, K., Belland Olsen, M., Ranheim, T., Sandanger, Ø., Dahl, T.B., Aukrust, P., Finsen, A.V., Yndestad, A., and Vinge, L.E. (2014). Toll-like receptor 9 mediated responses in cardiac fibroblasts. PLoS ONE *9*, e104398.

Raake, P.W., Vinge, L.E., Gao, E., Boucher, M., Rengo, G., Chen, X., DeGeorge, B.R., Jr., Matkovich, S., Houser, S.R., Most, P., et al. (2008). G protein-coupled receptor kinase 2 ablation in cardiac myocytes before or after myocardial infarction prevents heart failure. Circ. Res. *103*, 413–422.

Regnell, C.E., Hildrestrand, G.A., Sejersted, Y., Medin, T., Moldestad, O., Rolseth, V., Krokeide, S.Z., Suganthan, R., Luna, L., Bjørås, M., and Bergersen, L.H. (2012). Hippocampal adult neurogenesis is maintained by Neil3-dependent repair of oxidative DNA lesions in neural progenitor cells. Cell Rep. *2*, 503–510.

Reis, A., and Hermanson, O. (2012). The DNA glycosylases OGG1 and NEIL3 influence differentiation potential, proliferation, and senescence-associated signs in neural stem cells. Biochem. Biophys. Res. Commun. *423*, 621–626.

Rolseth, V., Krokeide, S.Z., Kunke, D., Neurauter, C.G., Suganthan, R., Sejersted, Y., Hildrestrand, G.A., Bjørås, M., and Luna, L. (2013). Loss of Neil3, the major DNA glycosylase activity for removal of hydantoins in single stranded DNA, reduces cellular proliferation and sensitizes cells to genotoxic stress. Biochim. Biophys. Acta *1833*, 1157–1164.

Sejersted, Y., Hildrestrand, G.A., Kunke, D., Rolseth, V., Krokeide, S.Z., Neurauter, C.G., Suganthan, R., Atneosen-Åsegg, M., Fleming, A.M., Saugstad, O.D., et al. (2011). Endonuclease VIII-like 3 (Neil3) DNA glycosylase promotes neurogenesis induced by hypoxia-ischemia. Proc. Natl. Acad. Sci. USA *108*, 18802–18807.

Sheng, Z., Oka, S., Tsuchimoto, D., Abolhassani, N., Nomaru, H., Sakumi, K., Yamada, H., and Nakabeppu, Y. (2012). 8-Oxoguanine causes neurodegeneration during MUTYH-mediated DNA base excision repair. J. Clin. Invest. *122*, 4344–4361.

Skarpengland, T., Dahl, T.B., Skjelland, M., Scheffler, K., de Sousa, M.M., Gregersen, I., Kuśnierczyk, A., Sharma, A., Slupphaug, G., Eide, L., et al. (2016). Enhanced base excision repair capacity in carotid atherosclerosis may protect nuclear DNA but not mitochondrial DNA. Free Radic. Biol. Med. *97*, 389–397.

Skarpengland, T., Laugsand, L.E., Janszky, I., Luna, L., Halvorsen, B., Platou, C.G.P., Wang, W., Vatten, L.J., Damås, J.K., Aukrust, P., et al. (2015). Genetic variants in the DNA repair gene NEIL3 and the risk of myocardial infarction in a nested case-control study. The HUNT Study. DNA Repair (Amst.) *28*, 21–27.

Spruijt, C.G., Gnerlich, F., Smits, A.H., Pfaffeneder, T., Jansen, P.W.T.C., Bauer, C., Münzel, M., Wagner, M., Müller, M., Khan, F., et al. (2013). Dynamic readers for 5-(hydroxy)methylcytosine and its oxidized derivatives. Cell *152*, 1146–1159.

Torisu, K., Tsuchimoto, D., Ohnishi, Y., and Nakabeppu, Y. (2005). Hematopoietic tissue-specific expression of mouse Neil3 for endonuclease VIII-like protein. J. Biochem. *138*, 763–772.

van den Borne, S.W.M., Diez, J., Blankesteijn, W.M., Verjans, J., Hofstra, L., and Narula, J. (2010). Myocardial remodeling after infarction: the role of myofibroblasts. Nat. Rev. Cardiol. *7*, 30–37.

Vaquerizas, J.M., Kummerfeld, S.K., Teichmann, S.A., and Luscombe, N.M. (2009). A census of human transcription factors: function, expression and evolution. Nat. Rev. Genet. *10*, 252–263.

Watson, C.J., Collier, P., Tea, I., Neary, R., Watson, J.A., Robinson, C., Phelan, D., Ledwidge, M.T., McDonald, K.M., McCann, A., et al. (2014). Hypoxia-induced epigenetic modifications are associated with cardiac tissue fibrosis and the development of a myofibroblast-like phenotype. Hum. Mol. Genet. *23*, 2176–2188.

Xu, X., Tan, X., Tampe, B., Nyamsuren, G., Liu, X., Maier, L.S., Sossalla, S., Kalluri, R., Zeisberg, M., Hasenfuss, G., and Zeisberg, E.M. (2015). Epigenetic balance of aberrant Rasal1 promoter methylation and hydroxymethylation regulates cardiac fibrosis. Cardiovasc. Res. *105*, 279–291.

Yndestad, A., Neurauter, C.G., Oie, E., Forstrøm, R.J., Vinge, L.E., Eide, L., Luna, L., Aukrust, P., and Bjørås, M. (2009). Up-regulation of myocardial DNA base excision repair activities in experimental heart failure. Mutat. Res. *666*, 32–38.